JGE (Jurnal Geofisika Eksplorasi)
Vol. 11 No. 02, July 2025 (122-134) https://doi.org/10.23960/jge.v11i2.492

DELINEATION OF ERUPTION PRODUCTS AND GEOTHERMAL PROSPECT ZONES IN MOUNT SLAMET, CENTRAL JAVA USING LANDSAT 8 AND GEOCHEMICAL DATA

DELINEASI PRODUK LETUSAN DAN ZONA PROSPEK PANAS BUMI DI GUNUNG SLAMET, JAWA TENGAH MENGGUNAKAN DATA LANDSAT 8 DAN GEOKIMIA

Hiskia Ulinuha Annisa[1*], Yogi Adi Prasetya[2], Zahra Nuraini Hadna[3], Puspita Dian Maghfira[4]

[1,2,3,4]Geological Engineering, University of Jenderal Soedirman, Purwokerto;

Received: 2025, June 13th
Accepted: 2025, July 15th

Keywords:
Mount Slamet;
Geothermal;
Geochemical;
Remote Sensing;
Landsat- 8.

Corespondent Email:
hiskia.annisa@unsoed.ac.id

How to cite this article:
Annisa, H.U., Prasetya, Y.A., Hadna, Z.N., & Maghfira, P.D. (2025). Delineation of Eruption Products and Geothermal Prospect Zones in Mount Slamet, Central Java using Landsat 8 and Geochemical Data. *JGE (Jurnal Geofisika Eksplorasi)*, 11(02), 122-134.

Abstract. Mount Slamet, located in Central Java, Indonesia, is one of the promising geothermal prospect areas due to its active volcanic system and distinct surface manifestations such as hot springs and altered grounds. This study aims to identify potential geothermal zones around Mount Slamet by integrating geochemical analysis and remote sensing data. Geochemical measurements from hot springs show temperatures ranging from 48–89 °C, pH values between 6.2–7.1, and elevated concentrations of SiO_2 (90–145 mg/L) and Cl^- (18–42 mg/L), indicating high-temperature fluid interaction. Remote sensing techniques, including thermal anomaly detection and alteration mineral mapping using multispectral and hyperspectral satellite imagery, were employed to delineate surface manifestations and hydrothermal alteration zones. The results indicate that the most prospective geothermal area is located in the southwestern part of Mount Slamet, characterized by strong thermal anomalies and geochemical signatures consistent with a high-enthalpy geothermal system. The integration of these methods provides a comprehensive assessment of geothermal potential, revealing key prospect areas with significant thermal anomalies and geochemical signatures indicative of a high-enthalpy geothermal system. These findings enhance understanding of Mount Slamet's geothermal potential and offer valuable.

Abstrak. *Gunung Slamet, yang terletak di Jawa Tengah, Indonesia, adalah salah satu daerah prospek panas bumi yang menjanjikan karena sistem vulkaniknya yang aktif dan manifestasi permukaan yang berbeda seperti mata air panas dan tanah yang diubah. Studi ini bertujuan untuk mengidentifikasi zona panas bumi potensial di sekitar Gunung Slamet dengan mengintegrasikan analisis geokimia dan data penginderaan jauh.*

Pengukuran geokimia dari mata air panas menunjukkan suhu berkisar antara 48–89°C, nilai pH antara 6,2–7,1, dan konsentrasi SiO_2 yang tinggi (90–145mg/L) dan Cl^- (18–42mg/L), yang menunjukkan interaksi fluida suhu tinggi. Teknik penginderaan jauh, termasuk deteksi anomali termal dan pemetaan mineral alterasi menggunakan citra satelit multispektral dan hiperspektral, digunakan untuk menggambarkan manifestasi permukaan dan zona alterasi hidrotermal. Hasilnya menunjukkan bahwa daerah panas bumi yang paling prospektif terletak di bagian barat daya Gunung Slamet, yang dicirikan oleh anomali termal yang kuat dan tanda-tanda geokimia yang konsisten dengan sistem panas bumi entalpi tinggi. Integrasi metode-metode ini menghasilkan penilaian potensi panas bumi yang komprehensif, mengungkap area prospek utama dengan anomali termal dan tanda-tanda geokimia yang signifikan, yang mengindikasikan sistem panas bumi berentalpi tinggi. Temuan ini meningkatkan pemahaman tentang potensi panas bumi Gunung Slamet dan menawarkan informasi berharga.

1. INTRODUCTION

Mount Slamet, an active Quaternary stratovolcano in Central Java, is composed of volcanic rock units including volcanic breccias, andesitic to basaltic andesite lava flows, and pyroclastic tuffs from past explosive eruptions. The presence of breccias and tuffs indicates a history of explosive activity, while the lava flows reflect effusive eruptions that have shaped the volcano's layered structure. This lithological diversity, along with surface geothermal manifestations and hydrothermal alteration zones, highlights the area's high potential for geothermal exploration (Harijoko et al., 2022; Nugraha et al., 2019).

Geothermal manifestations around Mount Slamet include hot springs located in the Guci and Baturraden areas. The Baturraden hot spring, particularly at Pancuran 7, is notable for the presence of extensive yellowish travertine deposits. The surface geothermal manifestations in the Guci area are characterized by bicarbonate-type fluids, while those in Baturraden exhibit chloride-bicarbonate fluid types (Harijoko & Juhri, 2017). These surface features are likely influenced by the area's permeability, which can be either primary, derived from rock formation processes (e.g., porosity, autobrecciated lava, lithological boundaries), or secondary, developed through tectonic deformation, rock dissolution, and hydrothermal brecciation (Anderson & Fairley, 2008).

Previous studies on Mount Slamet's geothermal potential have focused mainly on geological mapping and surface geochemical surveys (Harijoko & Juhri, 2017; Nugraha et al., 2019) but provide limited quantitative integration between geochemistry and remote sensing to delineate alteration zones and structural controls on geothermal systems. Furthermore, few studies have addressed how permeability structures, such as faults and fractures, influence hydrothermal alteration distribution. Geological manifestations in volcanic complexes can be observed from topographic expressions as an initial stage in volcanic geology research, in order to obtain results that represent actual field conditions. Optimizing topographic data and river drainage patterns, supported by Landsat imagery to delineate geological structures and volcanostratigraphic units, provides a highly relevant research approach for application under current conditions (Utama, 2020).

Therefore, this research aims to integrate geochemical analysis with remote sensing data to identify hydrothermal alteration zones and assess their relationship to structural features around Mount Slamet. Remote sensing makes it possible to map potential geothermal site for a large area effectively using thermal infrared (Isa

et al., 2020). This integrated approach is urgent because it enhances understanding of geothermal potential in one of Indonesia's largest and least-developed geothermal prospects, supporting future sustainable energy exploration and reducing dependence on fossil fuels. Distribution of geothermal potential areas can be effectively delineated using multi-sensor remote sensing techniques (Saepuloh et al., 2012).

2. GEOLOGICAL BACKGROUND

2.1. Research Area

Mount Slamet is located within the Sunda magmatic arc in Java Island, which was formed due to the subduction of the Indo-Australian plate with the Eurasian plate, which is included in the physiographic zone of the Central Mountain Zone (Bemmelen, 1949) which is dominated by young volcanic rocks of Quaternary age. Mount Slamet is classified as a stratovolcano, characterized by alternating explosive and effusive eruptions.

Mount Slamet is a volcanic complex that has two period eruptive phases, as indicated by the presence of both older and younger pyroclastic deposits. Mount Slamet is geologically divided into two parts, namely Old Slamet and Young Slamet. Old Slamet (OS) lies to the west, marked by rugged landscapes and deep valleys, with andesitic to basaltic-andesite rocks and pumice deposits (**Figure 1**). The products of Old Slamet volcanism include undefined volcanic rocks composed of breccias, lava, and tuff; hollow-textured andesitic lava flows; and lahar deposits within the Slamet Volcanic Complex (Assiddiqy et al., 2021). To the east is Young Slamet (YS), which consists mostly of basaltic rocks and scoria falls in the southeast (Prasetya et al., 2024). Lava flows linked to cinder cones were frequently generated by vent and flank eruptions of Young Mount Slamet during the Quaternary period. This cinder cone field suggests a substantial supply of basaltic magma, rising through surface fractures that acted as conduits (Assiddiqy et al., 2021).

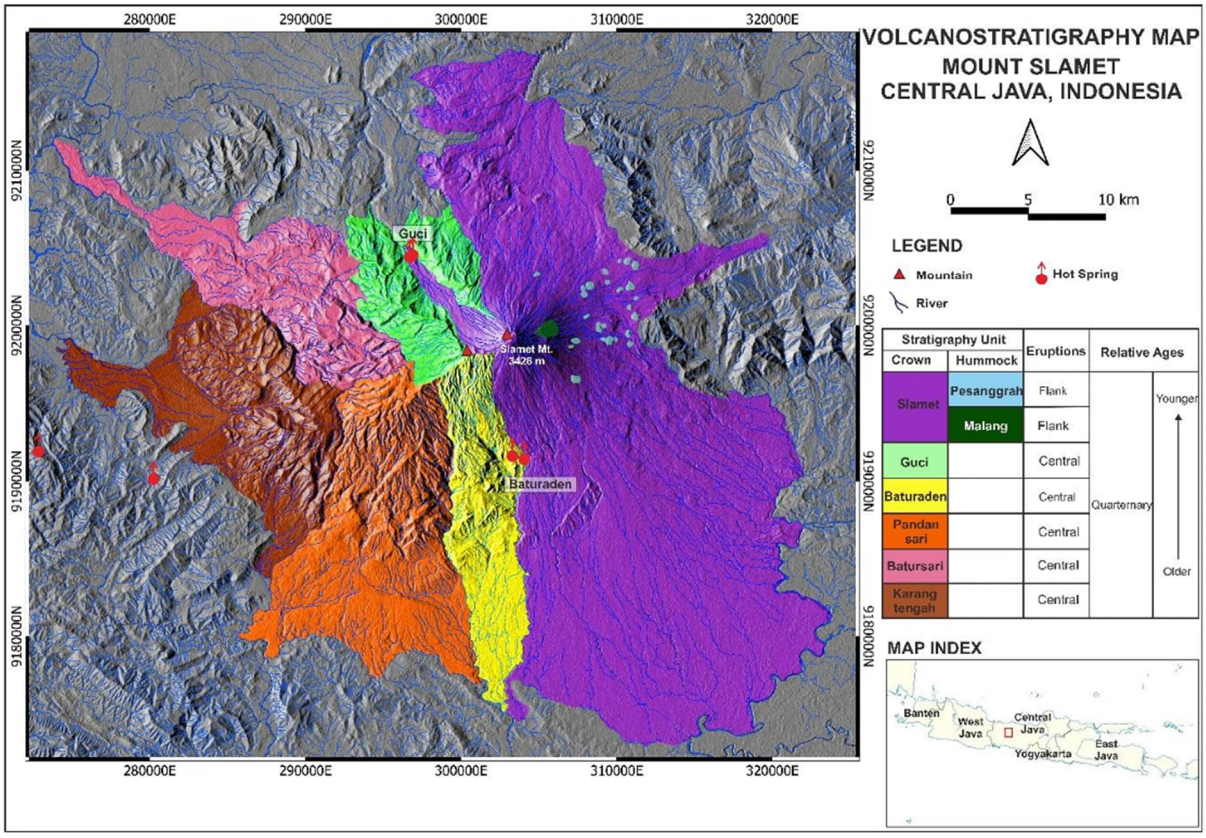

Figure 1. Volcanostratigraphy Map Mount Slamet, Central Java (Assiddiqy et al., 2021).

The study area is characterized by significant secondary permeability formed through various geological structures such as faults, fractures, hydrothermal breccias, and altered zones. These features result from both tectonic and volcanic activities, including the intrusion of magma and the circulation of hydrothermal fluids. Faults with orientations such as NW–SE and E–W serve as major conduits for geothermal fluid migration, while hydrothermal breccias and alteration zones enhance porosity and permeability at shallow depths. These secondary permeability features play a crucial role in channeling geothermal fluids from the heat source to surface manifestations, as observed in Baturraden and Guci hot springs. The presence of travertine deposits and bicarbonate to chloride-bicarbonate-type waters further confirms the influence of these geological structures on the geothermal system.

2.2. Geothermal Manifestation

Geothermal surface manifestations around Mount Slamet consist of several hot spring locations, distributed across Baturraden and Guci. In the Guci, located on the northern area of Slamet Volcano, there are three notable hot springs, namely Pancuran 13 hot spring, Cipanas Buaran hot spring, and Sigeong hot spring. On the southern, in the Baturraden area, two major hot springs can be found: Pancuran 5 and Pancuran 7, both of which are popular for their thermal water and travertine features (Harijoko & Juhri, 2017). These surface manifestations serve as important indicators of geothermal activity and provide valuable information for understanding the subsurface geothermal system of the region (**Figure 2**).

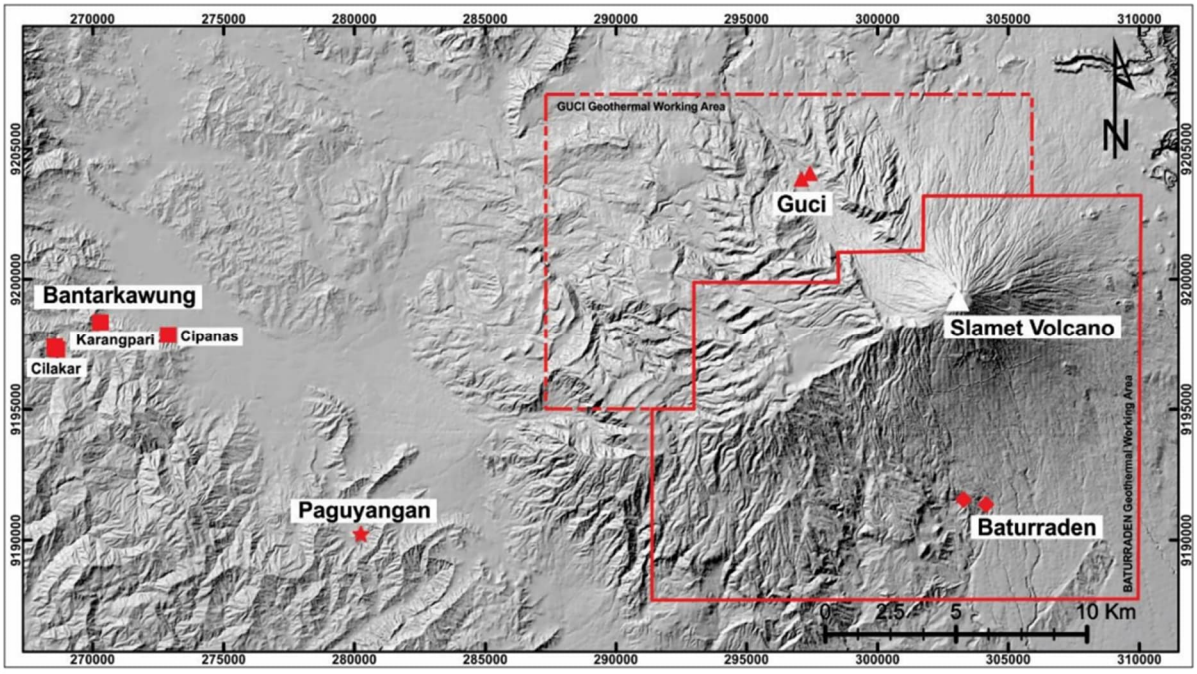

Figure 2. Map of Geothermal Manifestation Distribution in the Mount Slamet Region (Harijoko & Juhri, 2017).

3. RESEARCH METHODS

3.1. Geochemical Data

Geothermal waters around Mount Slamet exhibit various chemical types based on the concentrations of chloride (Cl^-), sulfate (SO_4^{2-}), and bicarbonate (HCO_3^-) ions (**Table 1**). The Baturraden hot springs are characterized as chloride-sulfate type, while the Guci hot springs represent a bicarbonate type.

The Bantarkawung hot springs fall into the chloride-bicarbonate type, and the Paguyangan hot springs are classified as chloride type (**Figure 3**). In contrast, all sampled cold spring waters predominantly show a bicarbonate composition, though some display slightly elevated chloride and sulfate concentrations. Several samples, including cold waters from Bantarkawung and thermal waters from Guci and Baturraden, exhibit geochemical signatures indicative of mixing between bicarbonate and chloride-sulfate water types (Harijoko & Juhri, 2017).

In addition to determining water types, reservoir temperatures were estimated using the Na-K geothermometer method (**Table 2**). The data reveal that the Bantarkawung area has a relatively low reservoir temperature, ranging between 57–58 °C. In contrast, the Baturraden area exhibits significantly higher estimated reservoir temperatures of approximately 280–290 °C, and the Guci area shows the highest range, estimated between 280–300 °C, suggesting a deeper and more active geothermal system in these regions.

Table 1. Geochemistry Data in Research Area (Harijoko & Juhri, 2017).

Location	Source	T (°C)	pH	Cl-	SO4	HCO3-	Li+	Na+	K+	Mg2+	SiO2	B	Ion Balance
Bantarkawung	River	27,4	6	5,07	28,6	197,64	0	11,56	0,92	6,9	17,85	0,34	-1
Bantarkawung	River	25,7	6	5,36	21,24	198,05	0	12,88	1,15	7,53	20,86	0,41	-2,5
Guci	Rain	22,4	7	3,31	20,72	84,38	10,02	4,3	7,05	7,05	54,59	0,48	-1,8
Bantarkawung	Rain	28,1	5	1,39	5,95	2,24	0,62	0,3	0,3	0,3	0	0,28	-12,4
Bantarkawung	Ground water	27,8	7	31,8	60,2	409,19	0	32,4	16,81	15,95	30,18	0,42	-2,4
Bantarkawung	Ground water	28,4	8	28,3	40,6	374,54	0	31,6	3,9	14,13	30,44	0,4	-2,4
Bantarkawung	Cold Spring	26,9	7	25,26	25,32	195,4	0	14	7,96	15,8	35,32	0,3	-1,6
Bantarkawung	Cold Spring	27,4	8	3,96	11,23	201,85	0	7,96	0,69	5,31	24,69	0,35	-2,5
Baturaden	Cold Spring	26,2	7	1,2	6,16	185,35	0,85	27,52	0,69	9,11	93,57	0,33	-1,6
Bantarkawung (Cipanas)	Hot Spring	21	6	13,36	14,68	70,15	0,01	12,48	4,27	0,67	48,02	0,37	-2,3
Bantarkawung (Cilakar)	Hot Spring	43	6	43,7	3,59	54,9	0,01	50,9	0,32	0,04	38,29	3,37	1,7
Bantarkawung (Cilakar)	Hot Spring	42,6	7	113	2,39	140,3	0,01	89	0,56	2,48	42,38	1,48	-1,5
Bantarkawung (Karangpari)	Hot Spring	43,1	7	120	1,2	132,17	0,01	94,9	0,59	1,86	44,15	1,64	-0,7
Baturaden (Pancuran 7)	Hot Spring	56	8	105	8,48	56,93	0,01	86,2	0,69	0,05	51,7	7,4	-2,1
Baturaden (Pancuran 3)	Hot Spring	50	7	754	609	687,27	0,67	389	76	185	169,14	4,4	-1,5
Guci (Pancuran 13)	Hot Spring	46	6	724	600	695,4	0,58	377	76,7	163,75	163,75	3,97	-1
Guci (Pengasihan)	Hot Spring	40,5	8,5	17,3	32,5	345,67	0,22	57,3	24,35	29,8	121,33	2,84	0,6
Paguyangan	Hot Spring	50,4	8	44,2	89	549,09	0,06	129	36,3	46,1	134,83	6,87	0,7

Table 2. Geothermometry of the Study Area Based on Quartz, Na/K, and K/Mg.

Hot Spring	Geothermometry			
	Quartz	Na/K (Fournier, 1979)	Na/K (Giggenbach, 1988)	K/Mg (Giggenbach 1986)
Pancuran 7	169	282	292	81

Pancuran 3	167	287	296	81
Pancuran 13	148	383	382	75
Pengasihan	155	325	331	80

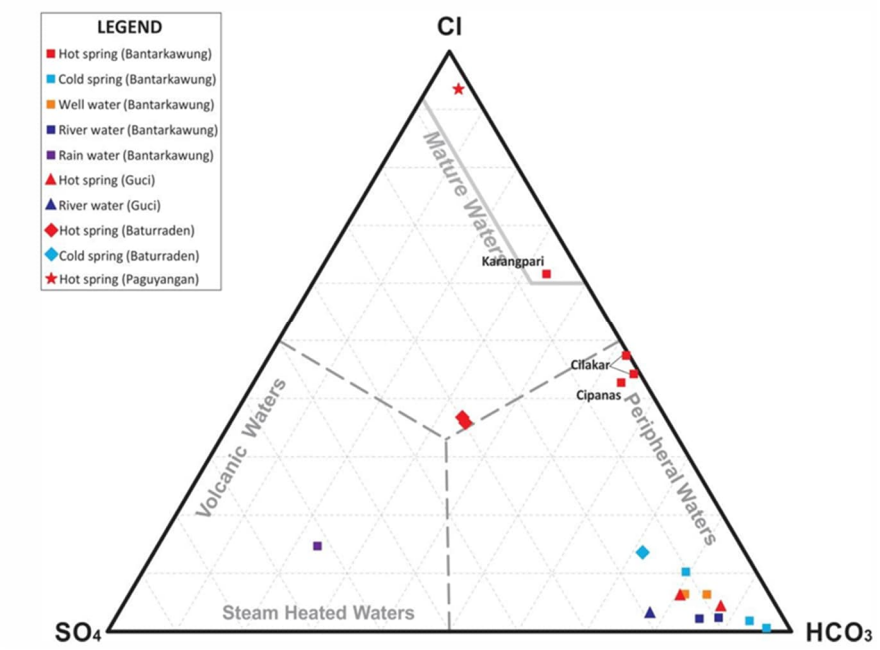

Figure 3. A ternary diagram showing the proportions of SO_4, Cl, and HCO_3 in hot spring and meteoric water samples from the study area (Harijoko & Juhri, 2017).

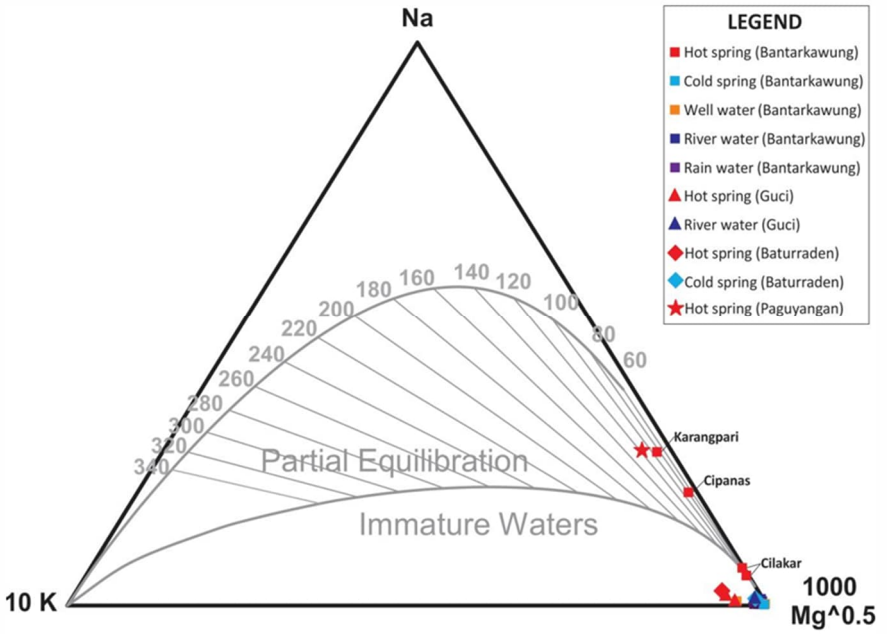

Figure 4. Ternary diagram illustrating the relative concentrations of Na, K, and Mg in hot spring and meteoric water samples collected from the study area. (Harijoko & Juhri, 2017).

3.2. Remote Sensing based on Landsat-8

Remote sensing in geology can be effectively utilized to identify and map lithological units, geological structures such as faults and folds, and formation boundaries. In the field of geothermal exploration, one of the key approaches to evaluating prospect potential is by observing the distribution of hydrothermal alteration minerals. The operation of this remote sensing method utilizes satellite imagery data in the form of Landsat-8 imagery and SRTM (Shuttle Radar Topography Mission) DEM (Siombone, 2022). This method offers a practical and efficient alternative to direct field surveys by utilizing remote sensing technology.

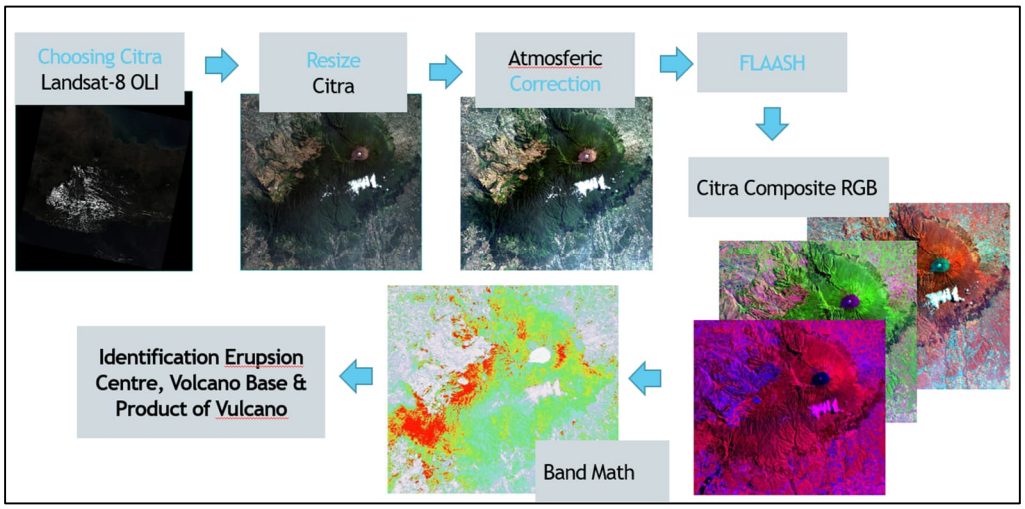

Figure 5. Workflow of Landsat-8 OLI image processing, including image selection, resizing, atmospheric correction (FLAASH), RGB composite generation, band ratio calculation, and interpretation of volcanic eruption centers, volcanic bases, and volcanic products.

In this study, Landsat-8 imagery was used. According to Saragih et al. (2015), Landsat-8 provides continuous, high-resolution multispectral data that covers the entire surface of the Earth. Its application is directed toward spectral analysis through data processing and interpretation across each spectral band. The type of data used from Landsat-8 (OLI/TIRS sensors) includes multispectral bands (Bands 1–7) and thermal bands (Bands 10 and 11), making it suitable for detecting surface mineralogical and thermal anomalies related to geothermal systems (Putri & Harianja, 2021). In the study by Maharani et al. (2021), Landsat-8 OLI imagery was used for NDVI and LST analysis, combined with DEM data for Fault Fracture Density (FFD) analysis, which proved effective in identifying geothermal potential on a regional scale. Landsat-8 image data processing was carried out using ENVI software. Remote sensing data processing in this study followed a structured workflow (**Figure 5**). Landsat-8 OLI imagery was selected and resized before applying atmospheric correction using the FLAASH module to minimize atmospheric effects. The corrected images were then combined into RGB composites to enhance surface feature visualization. Band ratio calculations (Band Math) were subsequently applied to highlight hydrothermal alteration zones, followed by the interpretation of volcanic eruption centers, volcanic bases, and volcanic products (**Figure 5**). To obtain optimal results, several processing steps were applied to the Landsat-8 data, including the following:

3.2.1. Atmosfer Correction

The purpose of this correction is to reduce atmospheric effects so that the imagery becomes more accurate and clearer, allowing surface features on the Earth to be better identified. This atmospheric correction process uses FLAASH (Fast Line-of-sight Atmospheric Analysis of Spectral Hypercubes), which is

capable of correcting images acquired from both hyperspectral and multispectral sensors within the visible to shortwave infrared wavelengths (up to 3 μm). FLAASH operates based on the MODTRAN4 radiative transfer code, rather than relying solely on interpolation from pre-existing data (Matthew et al., 2000).

FLAASH begins with a basic equation that describes the spectral radiance at a sensor pixel, L, which is valid for the solar wavelength range (ignoring thermal emission) and assumes flat surfaces with Lambertian reflectance or similar characteristics. The equation is given below (Matthew et al., 2000) :

$$L = \left(\frac{A\rho}{1-\rho_e S}\right) + \left(\frac{B\rho_e}{1-\rho_e S}\right) + L_a \quad (1)$$

ρ is the pixel surface reflectance. ρ_e is an average surface reflectance for the pixel and a surrounding region. S is the spherical albedo of the atmosphere. L_a is the radiance back scattered by atmosphere. A and B are coefficients that depent on atmospheric and geometric condition but not on surface.

The difference between ρ and ρ_e reflects the impact of the adjacency effect, which is the blending of radiance between nearby pixels due to atmospheric scattering. If you want to ignore this effect, you can assume ρ_e equals ρ. However, doing so may lead to major errors in reflectance, particularly at shorter wavelengths, in hazy conditions, or when there's a strong difference in material reflectivity in the scene. The parameters A, B, S, and L_a are derived from MODTRAN4 simulations, which take into account factors like the angle of the sensor and sun, the average elevation of the surface being measured, and predefined assumptions regarding atmospheric models, aerosol types, and visibility (Berk et al., 2003).

3.2.2. Composite Image and Band Math

After atmospheric correction was applied to the imagery, a composite image was generated using various RGB band combinations. *Band math* is an image analysis method used on Landsat 8 data to enhance spectral reflectance by emphasizing specific bands. In this study, the operation used is a division operation, also known as the band ratio method. To identify potential geothermal zones in the Mount Slamet area, the composite image was created using the formula (B2 + B3 + B5 + B7) / (B4 + B6), which is effective in highlighting zones of montmorillonite minerals. Montmorillonite is an alteration product of feldspar and amphibole minerals that have interacted with hydrothermal fluids. This mineral is indicative of the argillic alteration zone, which is commonly associated with geothermal systems.

4. RESULTS AND DISCUSSION

4.1. Deliniation of Volcano Product Based On Landsat-8

A false color composite of Mount Slamet and its surroundings (**Figure 6**), derived from corrected Landsat-8 imagery. On the left is the satellite image showcasing vegetation cover, volcanic landforms, and regional topography, while on the right is a spectral profile graph that illustrates the reflectance value across different wavelengths. This visualization serves as a fundamental basis for analyzing surface characteristics, particularly in geothermal and volcanic studies.

Based on **Figure 6**, it is evident that spectral brightness and reflectance values differ significantly compared to uncorrected data. This change highlights the importance of atmospheric correction, which removes the influence of atmospheric “noise” such as water vapor, aerosols, and gas scattering that can distort surface reflectance values. Without this correction, the data could misrepresent the actual spectral characteristics of ground materials, leading to inaccurate interpretations. The spectral profile graph on the right confirms this, showing a sharp increase in reflectance values across visible to near-infrared wavelengths after correction. This enhancement allows for more accurate identification of surface features, such as vegetation health, altered rocks, or volcanic deposits an essential step in remote sensing

analysis, especially in volcanic regions like Mount Slamet.

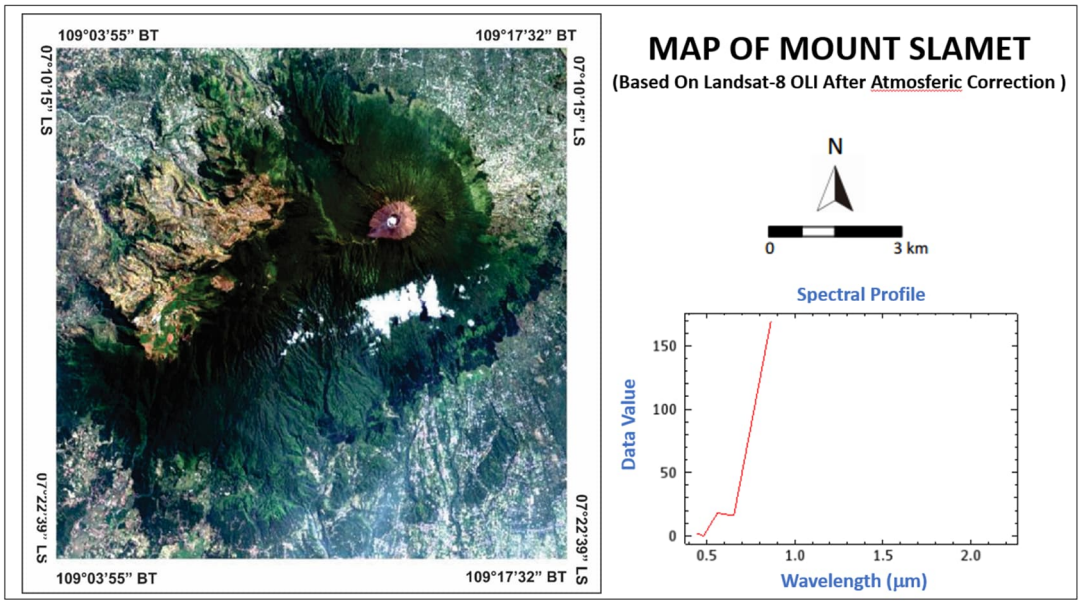

Figure 6. Map Of Mount Slamet Based on Landsat-8 OLI (Band 432).

The volcanic products of Mount Slamet are classified into two categories: Young Slamet Products and Old Slamet Products. **Figure 7**. interpreted that the volcanic products of young Mount Slamet are in the north, northeast, and southeast, while the products of old Slamet are in the west and north. The morphology of the young volcanic products is characterized by relatively smooth terrain surrounding the eruption center, where structural features are not yet well developed and the area shows low levels of erosion. These young deposits are typically in the form of shallow depressions that serve as lava flow paths. In contrast, the old volcanic products of Mount Slamet exhibit a more rugged morphology, marked by triangular facets and linear hill formations, which indicate a higher degree of erosion over time. These features suggest that the older volcanic units have been significantly shaped by erosional processes.

Overall, based on the band composite analysis (**Figure 7),** it can be observed that lava lithology typically exhibits a coarser surface texture, while pyroclastic rocks display a smoother morphological texture. The rugged morphology, associated with the older part of Mount Slamet, is characterized by steep slopes, deep valleys, and sharp, pointed peaks, and is predominantly found in the northwestern and southern sectors of the volcano. In contrast, the smoother terrain, representing the younger part of Mount Slamet, occupies the central area, consisting of irregular hilly landscapes with elongated ridges, rounded peaks, and broad valleys. Additionally, lava units can be identified by the presence of distinctive lava tongue formations at the tips of lava flows, which further assist in differentiating volcanic deposits in the region.

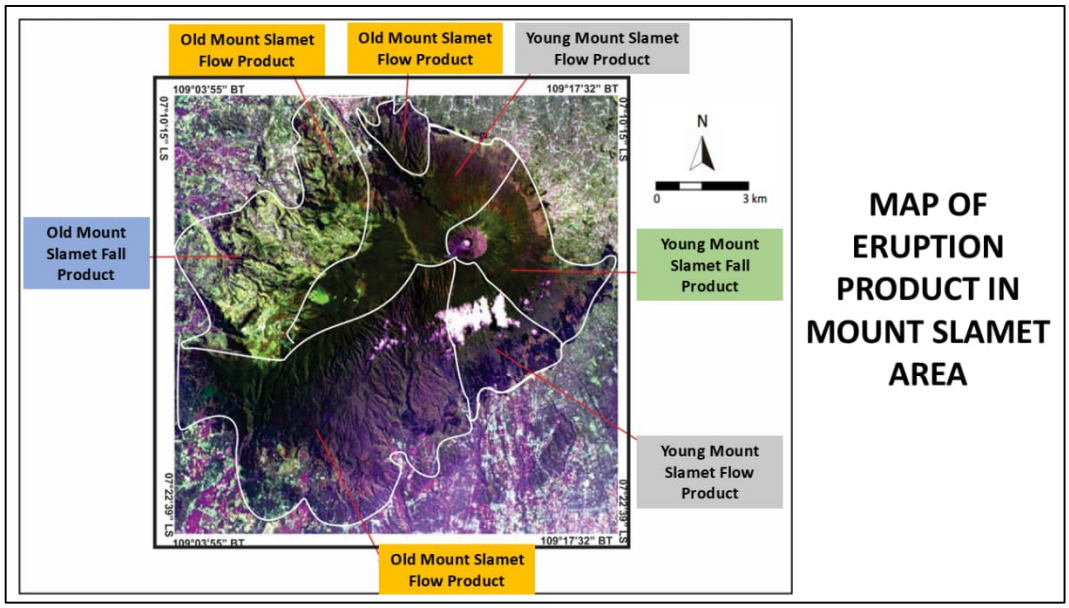

Figure 7. Map Of Eruption Product of Mount Slamet Area.

The spectral profile of eruption products from Mount Slamet (**Figure 8**), derived from Landsat 8 imagery, indicates that both lava and pyroclastic materials exhibit a consistent increase in reflectance from wavelengths of 0.5 µm to 0.85 µm. This pattern reflects the general characteristics of volcanic materials, which typically appear darker at shorter wavelengths and become more reflective at longer wavelengths. Interestingly, there is no significant difference in the spectral gradient between young and old lava, as well as between young and old pyroclastic deposits. This suggests that weathering or surface alteration processes have not substantially changed the spectral characteristics of these volcanic products, resulting in similar reflectance profiles regardless of their relative ages.

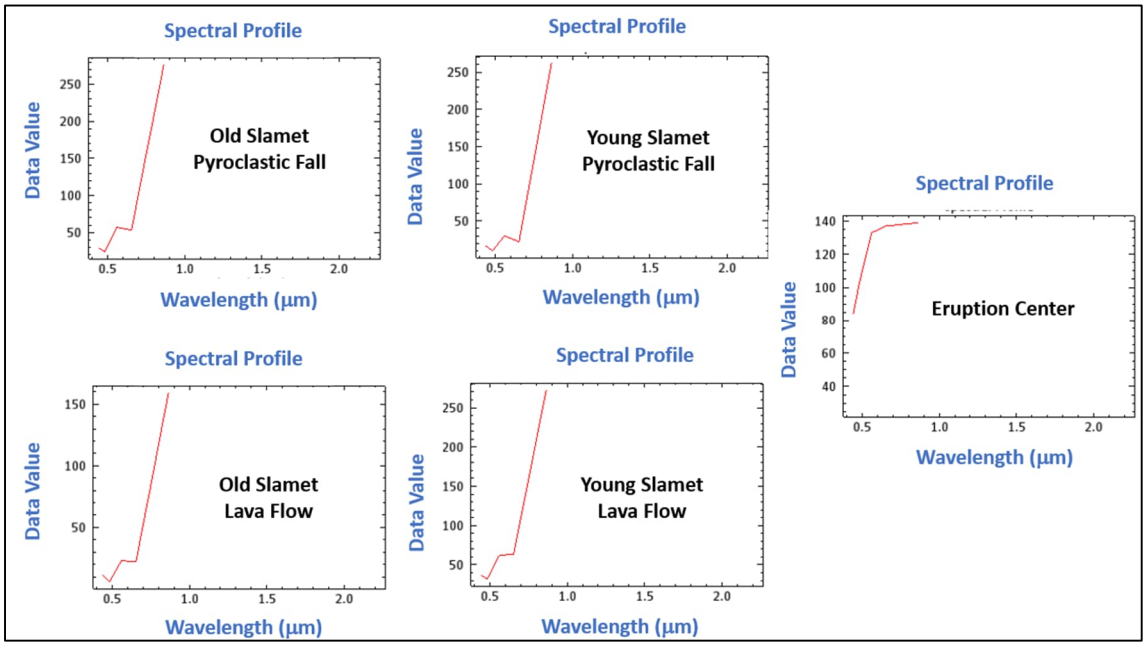

Figure 8. Spectral Profile Product Mount Slamet.

4.2. Geothermal Prospect Area Based On Remote Sensing and Geochemistry

Hydrothermal alteration zones serve as key indicators in geothermal exploration, as they reflect the interaction between hot geothermal fluids and surrounding host rocks. The presence of alteration minerals, particularly clay-rich assemblages, often corresponds to areas with high subsurface temperatures and fluid pathways. Therefore, mapping hydrothermal alteration zones is a crucial step in delineating potential geothermal prospect areas.

Hydrothermal alteration zones in the Mount Slamet area were analyzed using Landsat 8 OLI imagery through a band math approach to detect the presence of clay minerals, particularly montmorillonite. A specific band ratio formula, (Band 2 + Band 3 + Band 5 + Band 7) / (Band 4 + Band 6), was applied to enhance the spectral signature of montmorillonite, which is typically associated with argillic alteration in geothermal systems. Areas exhibiting high ratio values were interpreted as zones enriched in clay minerals, suggesting potential surface manifestations of hydrothermal activity. These zones are spatially correlated with known hot spring locations and structural lineaments, indicating their relevance as geothermal prospect areas in the Mount Slamet (**Figure 9**).

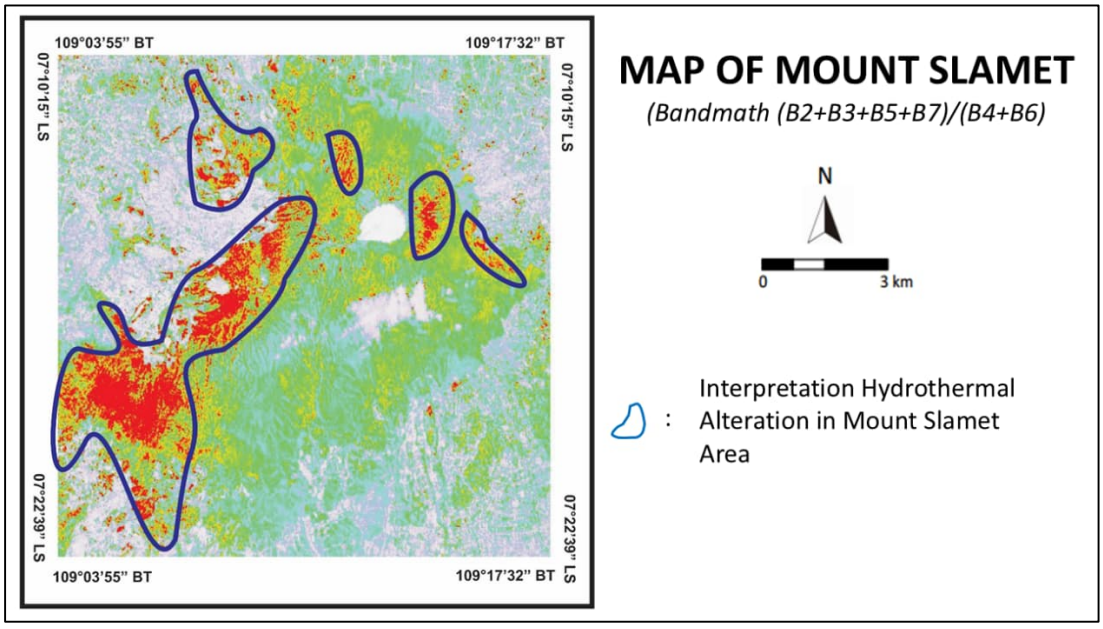

Figure 9. Map of hydrothermal alteration and structural lineaments in Mount Slamet area. Hydrothermal alteration zones (red areas) in the Mount Slamet area derived from band ratio (B2+B3+B5+B7)/(B4+B6). These alteration zones spatially coincide with structural features, including linear ridges and fractures, although individual ridge and fracture traces are not separately distinguished in this figure.

Interpretation of Landsat-8 imagery reveals that the dominant hydrothermal alteration zones are located in the southwestern part of Mount Slamet (**Figure 9**), which is very close to the geothermal manifestation area in Bantarkawung, spatially associated with older volcanic deposits. Additionally, alteration zones are also identified in the northwestern region, near the Baturraden hot spring manifestations. These alteration zones are further supported by the presence of structural features, such as linear ridges and fractures, observed within the same areas (**Figure 9**). These geological structures likely serve as conduits for ascending hydrothermal fluids, facilitating fluid–rock interaction. The

presence of fractures allows hot fluids to migrate to the surface and react with the surrounding host rocks, resulting in mineralogical changes that are manifested as alteration zones, detectable through spectral analysis.

Geochemical data from hot spring manifestations (**Table 1**) on the slopes of Mount Slamet indicate distinct fluid types. The Guci area is characterized by bicarbonate-type water, whereas the Baturraden springs exhibit a chloride–bicarbonate composition. According to Harijoko and Juhri (2017), these hot springs represent the discharge of a geothermal system beneath the volcano. The Baturraden fluids are interpreted as resulting from the mixing of volcanic fluids with meteoric water, as suggested by elevated Cl/SO_4 and Cl/B ratios, while the Guci system is primarily driven by volcanic processes with minimal surface water interaction. Reservoir temperatures, estimated using the quartz geothermometer and the Na–K–Mg ternary diagram, range between 150–170 °C, indicating a low-temperature geothermal system.

A comparison between remote sensing interpretation and geochemical data in the Mount Slamet area reveals a strong correlation in identifying geothermal prospect zones. Hydrothermal alteration zones detected through Landsat-8 imagery, particularly in the southwestern and northwestern sectors of the volcano, spatially coincide with geochemical anomalies such as elevated concentrations of dissolved ions in hot spring manifestations, especially in the Guci and Baturraden areas. These zones show high reflectance in SWIR bands, indicating the presence of alteration minerals like kaolinite and montmorillonite, which are characteristic of argillic alteration. The overlap between these spectrally identified zones and geochemical indicators such as high temperature, low pH, and elevated bicarbonate or chloride concentrations suggests a strong geothermal potential. Moreover, structural features such as linear ridges and fractures are present in these areas, implying that hydrothermal fluids migrated along these weak zones and altered the host rocks (**Figure 8**). The integration of remote sensing and geochemical data thus proves effective in delineating geothermal prospects, particularly in structurally controlled and older volcanic terrains of the Mount Slamet geothermal system.

5. CONCLUSION

Based on Landsat-8, volcanic products of Mount Slamet are classified into two categories: Young Slamet Products and Old Slamet Products. Volcanic products of young Mount Slamet are in the north, northeast, and southeast, while the products of old Slamet are in the west and north

Geochemical data from hot spring manifestations on the slopes of Mount Slamet indicate two distinct fluid types: bicarbonate-type water in Guci and chloride–bicarbonate-type water in Baturraden. The Baturraden hot springs are formed by mixing volcanic fluids with meteoric water, while the Guci system is mainly influenced by direct volcanic processes. Reservoir temperatures are estimated at 150–170 °C, indicating a low-temperature geothermal system.

The integration of Landsat-8 imagery and geochemical data effectively identifies geothermal prospect zones in Mount Slamet. Alteration zones in the southwest and northwest align with hot spring anomalies and structural features, indicating active fluid pathways. These overlapping indicators highlight the area's potential for further geothermal exploration.

REFERENCES

Anderson, S.R. & Fairley, J.P. (2008). Relating Permeability To Fault Structure in Basaltic Volcanic Rocks. *Journal of Geophysical Research: Solid Earth*, 113(B5), B05402. https://doi.org/10.1029/2007JB005422

Assiddiqy, M.H., Gati, R., Sibarani, B., & Suryantini (2021). Volcanostratigraphy Study of Slamet Volcano and The Implication to Its Early Stage

of Geothermal Exploration. *IOP Conf. Series: Earth and Environmental Science.* https://doi.org/10.1088/1755 1315/732/1/012009

Bemmelen, R.W.V. (1949). *The Geology of Indonesia (Vol. IA, General Geology).* The Hague: Government Printing Office.

Berk, A., Anderson, G.P., Acharya, P.K., Bernstein, L.S., Muratov, L., Lee, J., Fox, M., Adler-Golden, S.M., Chetwynd, J.H., & Matthew, M.W. (2003). *MODTRAN4 Version 3 Revision 1 User's Manual.* Air Force Research Laboratory, Hanscom Air Force Base, MA.

Harijoko, A. & Juhri, S. (2017). Cl/B Ratio of Geothermal Fluid Around Slamet Volcano, Jawa Tengah, Indonesia. *IOP Conference Series: Earth and Environmental Science*, 62, 012010. https://doi.org/10.1088/1755-1315/62/1/012010

Harijoko, A., Juhri, S., Taguchi, S., Yonezu, K., & Watanabe, K. (2022). Geochemical Indication of Formation Water Influx to The Volcanic Hosted Hot Springs of Slamet Volcano, Indonesia. *Indonesian Journal on Geoscience*, 7(1), 1–14. https://doi.org/10.17014/ ijog.7.1.1 14

Isa, M., Cesarian, D.P., Abir, I.A., Yusibani, E., Surbakti, M.S., & Umar, M. (2020). Remote Sensing Satellite Imagery and In-Situ Data For Identifying Geothermal Potential Sites: Jaboi, Indonesia. *International Journal of Renewable Energy Development*, 9(2), 237–245. https://doi.org/10.14710/ijred. 9.2.237-245.

Maharani, A., Salsanur, V., Hilal, A., & Aprilian, Y. (2021). Preliminary Interpretation For Geothermal Potential Area Using DEM and Landsat OLI 8 in Mount Endut. *Bulletin of Scientific Contribution*, 19(1).

Matthew, M.W., Adler-Golden, S.M., Berk, A., Felde, G.W., Anderson, G.P., Gorodetzky, D., Paswaters, S., Shippert, M., & Hoke, M.L., (2000). Atmospheric Correction of Hyperspectral Data Using FLAASH and MODTRAN4. In: *Proceedings of the SPIE, Algorithms for Multispectral, Hyperspectral, and Ultraspectral Imagery* VI, 4049, pp. 14–21.

Nugraha, P., Sari, D., & Hidayat, T. (2019). Geothermal Geochemical Study of Slamet Volcano. *Indonesian Journal of Geology,* 14(2), 121–134

Prasetya, Y.A., Gibran, A.K., Aziz, M., & Siswandi. (2024). Petrology, Geochemistry, and Magma Evolution of Basaltic Rocks of Baturraden Area, Central Java, Indonesia. *Journal of Geoscience, Engineering, Environment, and Technology,* 9(4). https://doi.org/10.25299/jgeet.2024.9.04.17882

Putri, D.A.B. & Harianja, A.K. (2021). Identifikasi Prospek Panas Bumi Radiogenik Menggunakan Landsat-8 dan Gravitasi di Daerah Permis. *JGE (Jurnal Geofisika Eksplorasi),* 7(1), 52–70. https://doi.org/10.23960/jge.v7i1.115

Saepuloh, A., Urai, M., Sumintadireja, P., & Suryantini (2012). Spatial Priority Assessment of Geothermal Potentials Using Multi-Sensor Remote Sensing Data and Applications. Proceedings of the *1st ITB International Geothermal Workshop* 2012, Bandung.

Saragih, H., Sihotang, M., Hutabarat, D., & Sinaga, A. (2015). Pemanfaatan Citra Satelit Landsat-8 Untuk Identifikasi Potensi Panas Bumi Berdasarkan Analisis Spektral dan Anomali Termal. Jurnal Geosains, 11(2), pp.75–85.

Siombone, S.H. (2022). Analisis Suhu Permukaan dan Kondisi Geomorfologi Kawasan Geotermal Tehoru Menggunakan Landsat-8 dan DEM. *JGE (Jurnal Geofisika Eksplorasi),* 08(03), 210-224. https://doi.org/10.23960/ jge.v8i3.243

Utama, H.W. (2020). Struktur Geologi dan Vulkanostratigrafi; Analisis Model Elevasi Digital dan Citra Landsat 8. *JGE (Jurnal Geofisika Eksplorasi),* 6(2), 156-168. https://doi.org/10.23960/jge.v6i2.80